Chapter-5

Demonstration of Auxochromic Effects of Alicyclic Amines on Naphthalimide and Nitrobenzoxadiazole Fluorophores

5. Demonstration of Auxochromic Effects of Alicyclic Amines on Naphthalimide and Nitrobenzoxadiazole Fluorophores

5.1. Background and Rationale

In our previous chapter, we delved into the auxochromic effects of alicyclic amines on coumarin fluorophores. We discovered that incorporating these cycloalkylamines has broadened the range of luminogenic coumarins beyond the typical 7-hydroxy and 7-amino analogues (**1a-1b**) for the development of modern fluorescent probes. Upon analyzing the synthesized derivatives, we found that compounds **3** and **4** have the highest quantum yields in the series, slightly surpassing the standard compound **2**. Upon further analysis, it has been discovered that the cycloalkylaminated derivatives of coumarin display exceptional photostability, pH stability, cell permeability, and biocompatibility, making them highly promising for use in biological imaging. These alicyclic amines, especially cyclobutylamine and cyclopentylamine, exhibit all the advantages of azetidine auxochrome and also contain a nitrogen center for further functionalization into biochemical-detecting probes.

Delighted by the scope of cycloalkylamine auxochromes, we then sought to explore the versatility and reproducibility of its effects when integrated into other fluorophores. We anticipate that cycloalkylamine rings could modulate the photophysical properties of other fluorophores in a similar manner as in coumarins with future applications in bioimaging. The applications of 1,8-naphthalimide [1–3] and 4-nitrobenzoxadiazole-based chemosensors [4] in bioimaging is extensively reported in the literature. In this chapter, we carried out the installation of cycloalkyl amine rings as electron donors in naphthalimide (**5a**-**5e**) and nitrobenzoxadiazole (**6a**-**6e**) fluorophores (figure 5.1) and compared them with their azetidine counterparts **5** and **6**, respectively, which have been reported to have very high quantum yields.[5]

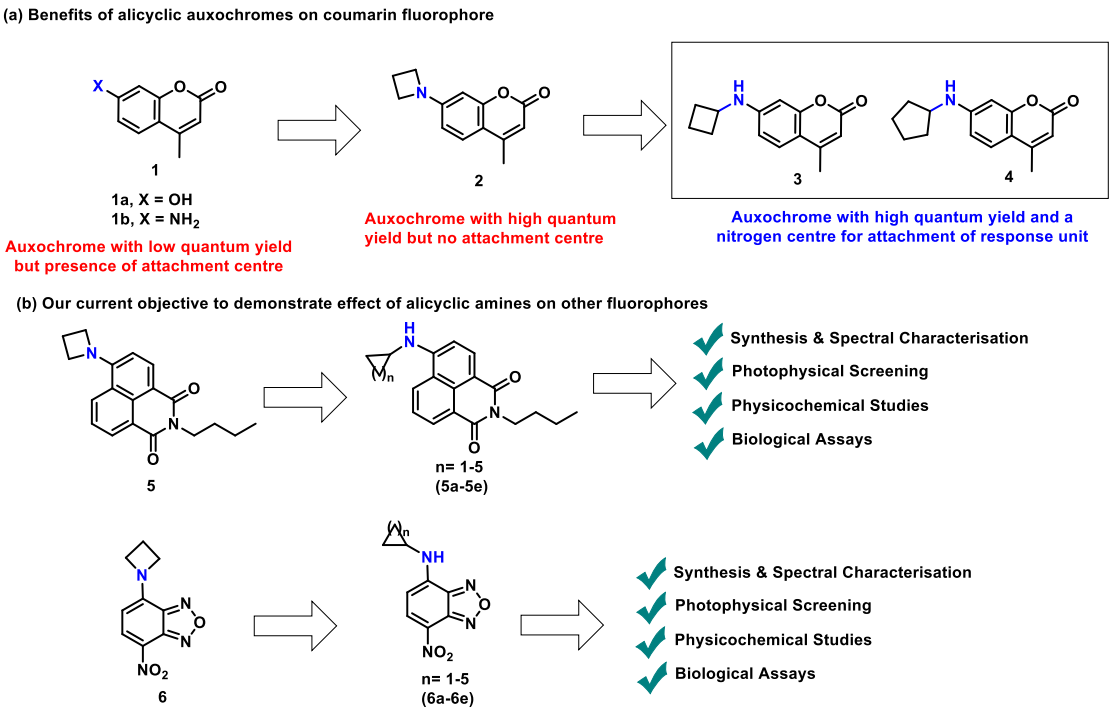

Figure 5.1. (a) Demonstration of benefits of cycloalkyl amine auxochromes on coumarin fluorophore as compared to traditional hydroxyl (**1a**), amine (**1b**) and azetidine (**2**) auxochromes. (b) Current objective depicting the evaluation of alicyclic auxochromes on naphthalimide (**5a-5e**) and nitrobenzoxadiazole (**6a-6e**) fluorophores in comparison to their corresponding azetidinylated counterparts (**5** and **6**, respectively), treated as standards.

5.2. Results and Discussion

5.2.1. Synthesis of target molecules

Synthetic routes for target structure (**5a-5e** and **6a-6e**) and standard compounds (**5** and **6**) are given in schemes 5.1 and 5.2. Compounds **5** and **5a-5e** were prepared from commercially available precursor, 4-bromo-1,8-naphthalic anhydride (**A**). Precursor **A** was refluxed with *n*-butylamine in the presence of ethanol for 2 h, which resulted in the formation of 6-bromo-2-butyl-1*H*-benzo[*de*]isoquinoline-1,3(2*H*)-dione (**B**) in 75 % yield. Compound **B** undergoes nucleophilic aromatic substitution (S_NAr) with azetidine and cycloalkyl amines, when refluxed in the presence of triethylamine (Et_3N) in dimethylsulfoxide (DMSO) for 6 h and give the product **5** in 85% yield and **5a-5e** in 68-78 % yields (scheme 5.1).

Scheme 5.1. Synthesis of naphthalimide derivatives 5 and 5a-5e.[a]

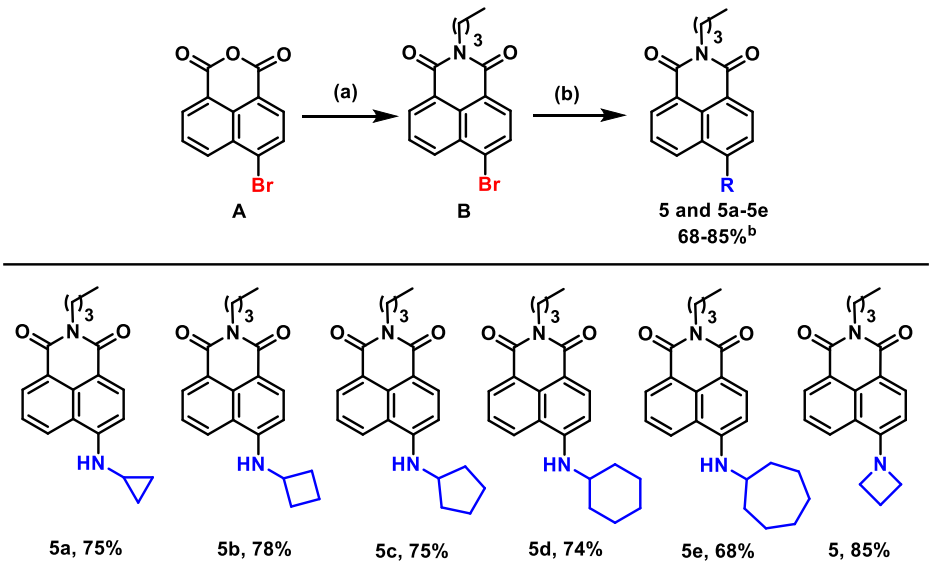

[a]**Reaction conditions**: **(a) A** (6 mmol), *n*-butylamine (1.5 equiv.), EtOH (7 mL), refluxed at 80 °C for 2h; **(b) B** (0.9 mmol), triethylamine (1.5 equiv.) and amines (1.5 equiv.), DMSO (2 mL), heated at 110 °C for 6 h. [b]Isolated yields.

Compounds **6** and **6a-6e** were prepared from commercially available precursor, 4-chloro-7-nitrobenzo[*c*][1,2,5]oxadiazole (**C**). Precursor **C** was refluxed with azetidine and cycloalkyl amines in the presence of Et_3N and DMSO for 2 h to get product **6** in 67% yield and **6a-6e** in 60-69 % yields (Scheme 5.2).

Scheme 5.2. Synthesis of 4-nitrobenzoxadiazole derivatives 6 and 6a-6e.[a]

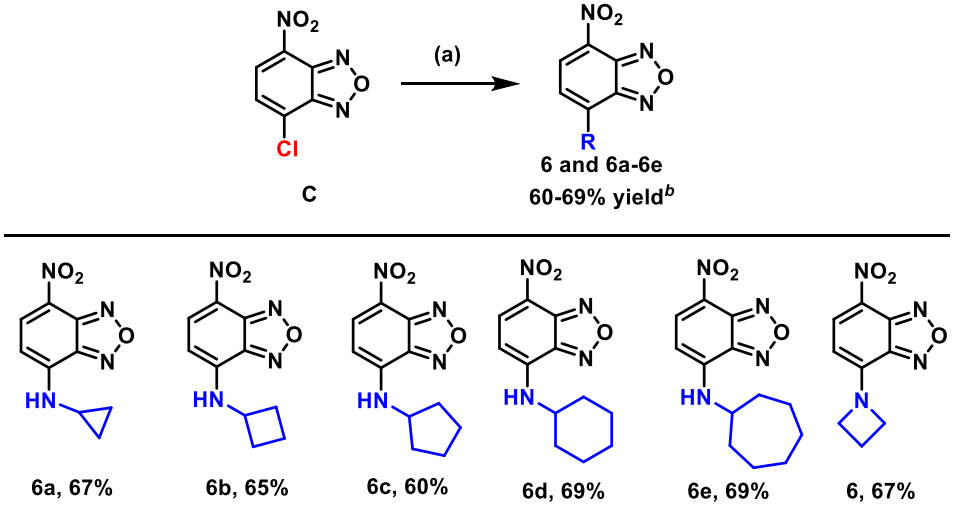

[a]**Reaction conditions**: (**a) C** (1 mmol), triethylamine (1.5 equiv.) and the alicyclic amines/azetidine (1.5 equiv.), DMSO (2 ml), reflux for 2h. [b]Isolated yields.

5.2.2. Photophysical Characterization of target molecules

After the successful synthesis of the target compounds (**5a-5e** and **6a-6e**) and standard compounds (**5** and **6)**, we then turned to investigate the photophysical behaviors of synthesized compounds (table 5.1). The absorption maxima for compounds **5a-5e** and **5** in PBS were recorded at 444-454 nm and 462 nm, respectively (table 5.1, figure 5.2). The fluorescence emission maxima for compounds **5a-5d** were recorded at 549-553 nm, similar to the emission wavelength of the standard compound **5** (λ_{em}= 556 nm) (table 5.1, figure 5.2). The emission wavelength of **5a-5d** showed that the emission wavelengths are independent of the *N*-cycloalkylated ring size. Interestingly, 7-membered cycloalkyamine derivative **5e** (λ_{em} = 541 nm) showed sudden fall in the emission wavelength. Absolute quantum yields (φ) of the compounds **5** and **5a-5e** in PBS were measured using an integrating sphere (table 5.1). Comparing **5a** and **5b**, an increase in ring size from cyclopropyl (**5a**, $\varphi \approx 0.091$) to cyclobutyl (**5b,** $\varphi \approx 0.207$) resulted improvement in quantum yield**.** Further, expansion of ring size (**5b-5d**) from cyclobutyl to cyclohexyl, enhanced the flexibility in ring system, which ultimately resulted in a gradual decrease in quantum yield. Interestingly, compound **5e** ($\varphi_f \approx 0.103$) having cycloheptyl ring showed quantum yield higher than **5d** ($\varphi_f \approx 0.097$) having cyclohexyl ring. This could be attributed to the larger hydrophobicity of the cycloheptyl ring, which minimizes the hydrogen bond formation of **5e** with water and thus protects the fluorescence. However, decreased water solubility of **5e** owing to larger hydrophobicity makes it unsuitable for bioimaging. Among the synthesized cycloalkylamine naphthalimides (**5a-5e**), compound **5b**, having cyclobutylamino auxochrome, showed quantum yield and brightness higher than standard compound **5**. Next, we examined the photophysical properties of NBD derivatives **6** and **6a-6e.** The absorption maxima for compounds **6a-6e** and **6** were observed at 479-492 nm

and 500 nm, respectively (Table 5.1, figure 5.2). Azacyclic NBD **6** (λ_{em}= 566 nm) displayed a fluorescence emission wavelength larger than alicyclic NBD **6a-6e** (λ_{em}= 548-552 nm) (Fig. 2b). The effect of cyclic ring size on the light emitting properties of NBD fluorophores **6a-6e** followed a similar trend as that of naphthalimide fluorophores **5a-5e**. Among synthesized cycloalkylamine NBD dyes **6a-6e**, compound **6b** having cyclobutylamino auxochrome exhibited quantum yield and brightness higher than standard compound **6**.

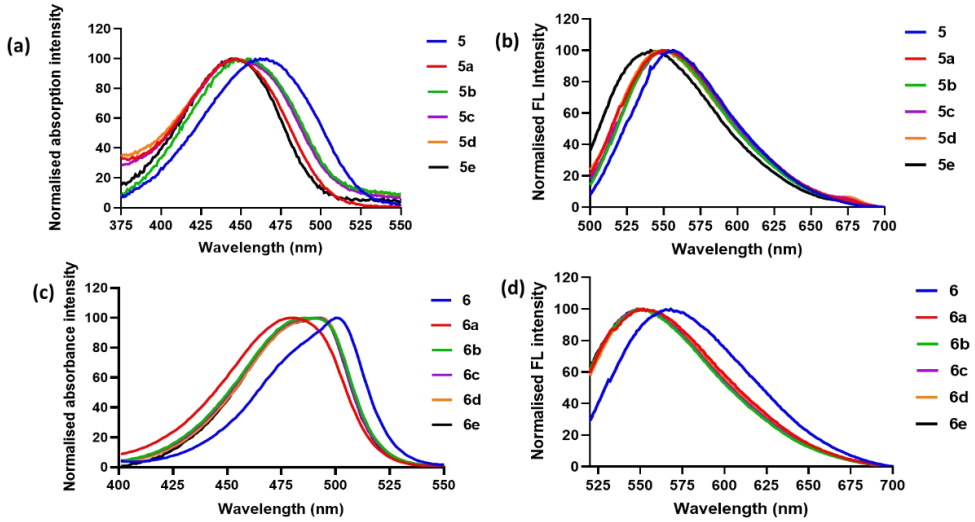

Figure 5.2. (a,b) Normalised absorption and fluorescence emission peaks of compounds **5a-5e** in PBS in comparison to **5**; (c,d) Normalised absorption and fluorescence emission peaks of compounds **6a-6e** in PBS in comparison to **6**.

Table 5.1. Photophysical properties of synthesized compounds in PBS.

Compound	**λ_{max} (abs)^a**	**λ_{max} (em)^b**	**Stokes Shift**	**ε^c ($M^{-1}cm^{-1}$)**	**φ_f ^{d}**	**Brightness ($M^{-1}cm^{-1}$)**
5a	448	553	105	3743	0.091	341
5b	454	549	95	14370	0.207	2979
5c	447	549	102	5976	0.144	860
5d	448	549	101	5996	0.097	581.6
5e	444	541	97	11970	0.103	1232
5	462	556	94	14700	0.190	2793

6a	479	552	73	25610	0.013	332
6b	485	551	66	41690	0.039	1626
6c	492	548	56	20380	0.032	658
6d	493	548	58	26760	0.032	851
6e	492	548	56	27040	0.030	803
6	500	566	66	39400	0.034	1305

[a] λ_{max} (abs) = absorption maxima (nm); [b] λ_{max} (em) = emission maxima (nm); [c] ε molar absorptivity; [d]Absolute quantum yield

5.2.3. Theoretical explanation of findings using DFT studies

To study the electronic effect of azetidine and cyclobutylamine on naphthalimide dyes **5** and **5b,** we have performed quantum chemical studies utilizing DFT/B3LYP 6-31++G(d,p) and TD-DFT/B3LYP 6-31++G(d,p) methods. Theoretical calculations for ground state (S_0) geometry optimization have given us the most stable and minimal energy conformations of compounds **5, 5b, 6** and **6b**. Further, singlet excited state (S_1) energy calculations of compounds **5** and **5b** show significant differences in the alignment of azetidine and cyclobutylamine rings with the naphthalimide core (figure 5.3a). The side view of compound **5** displays a flat conformation of azetidine along with co-planarity with the naphthalimide, ensuring an uninterrupted flow of electrons with minimal steric repulsion and elevated quantum yield (figure 5.3b). On the other hand, the side view of compound **5b** shows up-down conformation of the geometrically constrained cyclobutyl amine ring with the naphthalimide (figure 5.3b). Hence, rigid conformation and electron-donating ability of cyclobutylamine auxochrome contributes to the enhanced quantum yield of compound **5b,** despite lack of co-planarity to the fluorophore. The electronic distributions of compounds **5** and **5b** and their HOMO and LUMO energy gaps (figure 5.3c) show that the electron density of the HOMO of **5** is delocalized on the naphthalimide scaffold and the azetidine moiety (mainly on the nitrogen atom and its two arms). The butyl group on the naphthalimide ring does not participate in electronic distribution. In LUMO, the electron

density on azetidine moves to the naphthyl ring system and extends up to imide moiety. The electronic distribution in HOMO and LUMO of compound **5a** showed a similar trend as that of **5,** showcasing the push-pull effect on the D-π-A system of the established fluorophore. The HOMO–LUMO energy band gaps in compounds **5** and **5b** were found to be 3.209 eV and 3.267 eV, respectively. The shorter band gap in **5** (λ_{abs} = 462 nm) compared to **5b** (λ_{abs} = 454 nm) corresponds to a redshift in the absorption maximum of the former. Furthermore, optimization calculations on the S_1 state geometry led us to find the electronic energy distribution of compounds **5** and **5b** after emission when they return to their ground state (S_0). The HOMO–LUMO energy gap in compound **5** (2.051 eV) was found to be somewhat lesser than that of **5b** (2.953 eV) due to the red shift in the emission maximum of **5** (λ_{em} = 556 nm) with respect to **5b** (λ_{em} = 549 nm) (see appendix).

Similarly, singlet excited state (S_1) molecular structures of compounds **6** and **6b** show coplanar and up-down conformations of azetidine and cyclobutylamine**,** respectively (Fig. 3). The HOMO-LUMO electron distribution of **6** and **6b** show a significant delocalization of the electronic density from the respective electron-donating azetidine and cyclobutylamine to the NBD scaffold, displaying a significant push-pull effect of the NBD fluorophore. The blue shift of absorption wavelength of **6b** (λ_{abs} = 485 nm) in comparison to **6** (λ_{abs} = 500 nm) is consistent with their theoretically calculated HOMO-LUMO band gaps, 3.192 eV and 3.107 eV, respectively (figure 3c). Further, the HOMO–LUMO energy gap obtained from optimization calculations on the S_1 state geometry of compounds **6** (2.855 eV) and **6b** (2.90 eV) are consistent with the red shift in the emission maximum of **6** (λ_{em} = 566 nm) with respect to **6b** (λ_{em} = 551 nm) (see appendix).

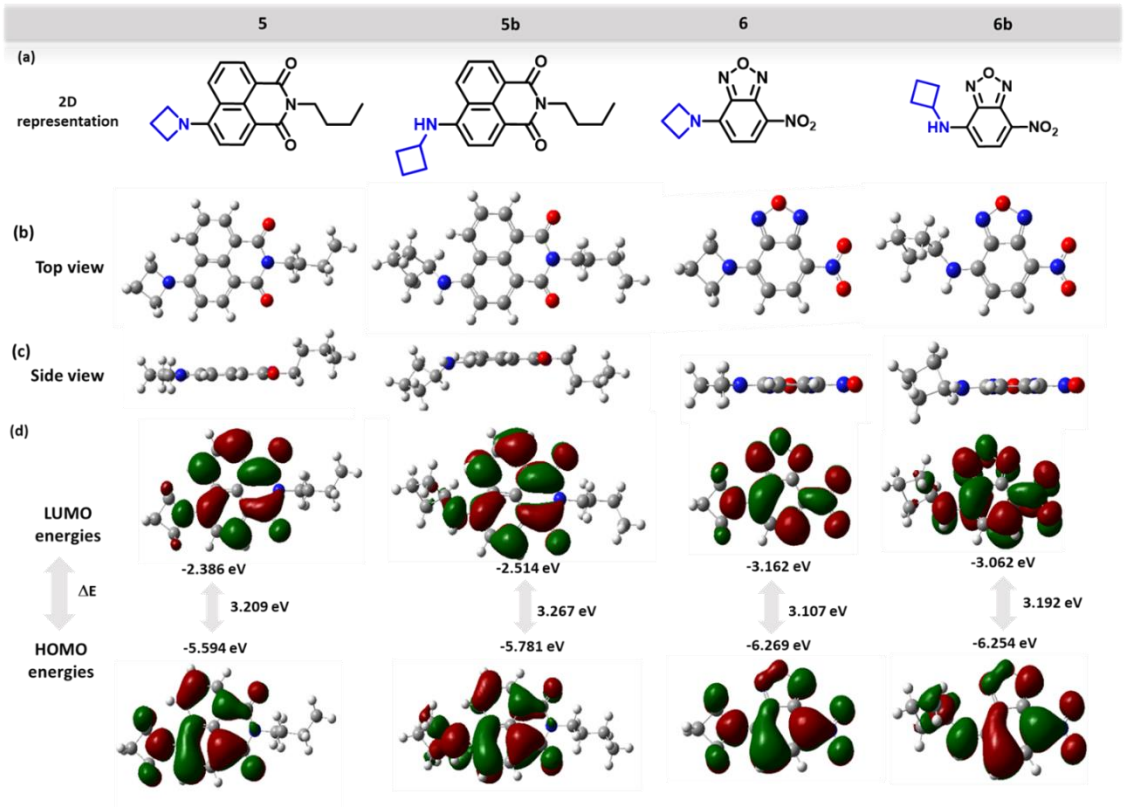

Figure 5.3. Illustrations of (a) 2D representation, (b) top view and (c) side view of theoretically optimized molecular structures of **5**, **5b**, **6** and **6b** in water in singlet excited state (S_1); (d) HOMO (highest occupied molecular orbital) and LUMO (lowest unoccupied molecular orbital) electron densities of **5**, **5b**, **6** and **6b** in water in singlet excited state (S_1) calculated based on the optimized molecular structures in the S_0 state.

5.2.4. pH Stability and Photostability Studies of molecules

The effect of pH changes on the stability of cyclobutylamine derivatives (**5b** and **6b**) was important for evaluation due to their prospective bioimaging applications. To our pleasure, no significant variation in the fluorescence intensity of compounds **5b** and **6b** were obtained over a pH range of 4-7 (figure 5.4a-b), which reflects the stability of the cyclobutylamine auxochrome in a physiological pH range. Experiments to evaluate the photostability of compounds **5**, **5b**, **6** and **6b** were carried out using time-dependent photobleaching method and the obtained results were compared to a standard dye **coumarin 6** (λ_{ex}: 457 nm; λ_{em}: 501

nm) which is popularly used in cell labelling and imaging studies. The compounds (dissolved in DMSO/PBS-20:80) were subjected to continuous exposure to white light for 5h. The results indicated that the photostabilities of compounds **5b** and **6b** are relatively better than their azetidinyl counterparts, **5** and **6**, respectively (figure 5.4c-d).

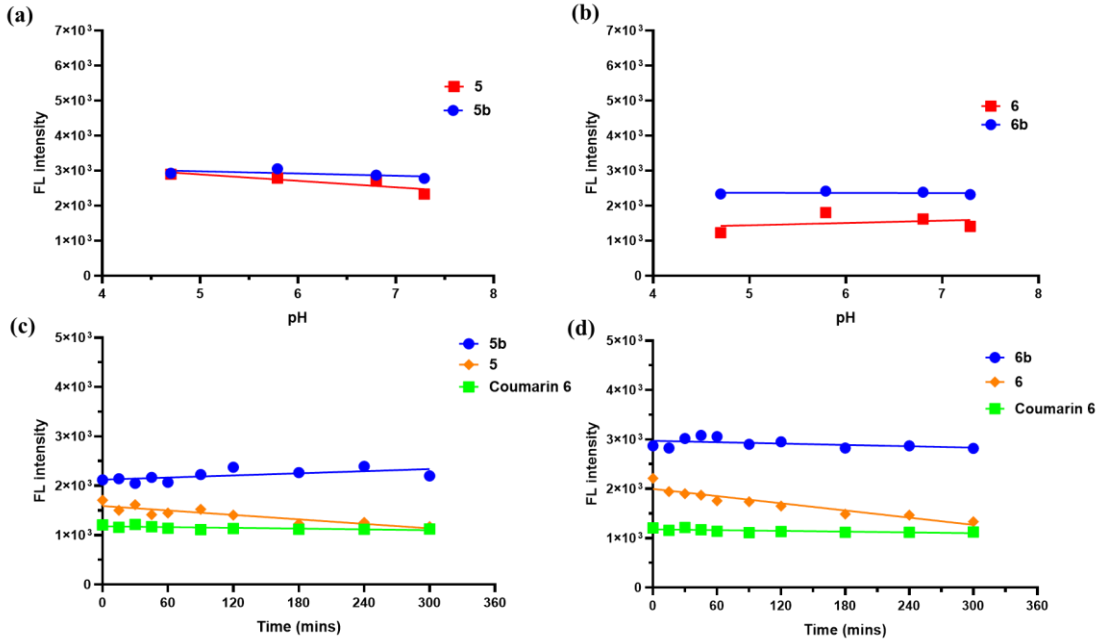

Figure 5.4. (a, b) Evaluation of the stability of compounds **5b** and **6b** in response to pH as compared to their reference standards **5** and **6**, respectively; (c, d) Photostability tests of compounds **5b** and **6b** in comparison to standards **5** and **6,** respectively, using **coumarin 6** as the reference dye.

5.2.5. Biocompatibility Assay of molecules in both cancer and non-cancer cells

Prior to bioimaging, we investigated the cytotoxicity of naphthalimide dyes (**5** and **5b**) and NBD dyes (**6** and **6b**) by MTT assays on the MDA-MB-231 breast cancer cell line (Fig. 5.5a-b) and non-cancerous HEK-293 human embryonic kidney cell line (figure 5.5c-d). Cytotoxicity results in MDA-MB-23 cells demonstrated that compounds **5** and **5b** exhibited more than 90% viability at low concentrations (up to 25 µM), but at higher concentrations (50 µM-100 µM), **5b** was found to be safer than standard 5 (figure 5.5a). Compounds **6** and **6b** exhibited

more than 80% of cell viability at higher concentrations (50-100 μM), suggesting minor cytotoxicity in cancer cells. However, **6b** was found to be safer than standard 6 at all measured concentrations (figure 5.5b). The cytotoxicity assay in the HEK-293 cell line (figure 5.5c-d) revealed that compounds **5**, **5b**, **6**, and **6b** exhibited more than 90% cell viability up to 50 μM concentration, but at higher concentrations (75 μM-100 μM), reference compounds **5** and **6** having azetidine auxochrome were found to be safer than compounds **5b** and **6b** having cyclobutyl amine auxochrome. Cytotoxicity studies imply significant biocompatibility of the synthesized dyes **5b** and **6b** in both cancer and non-cancer cell lines and, hence, their potential application in bioimaging.

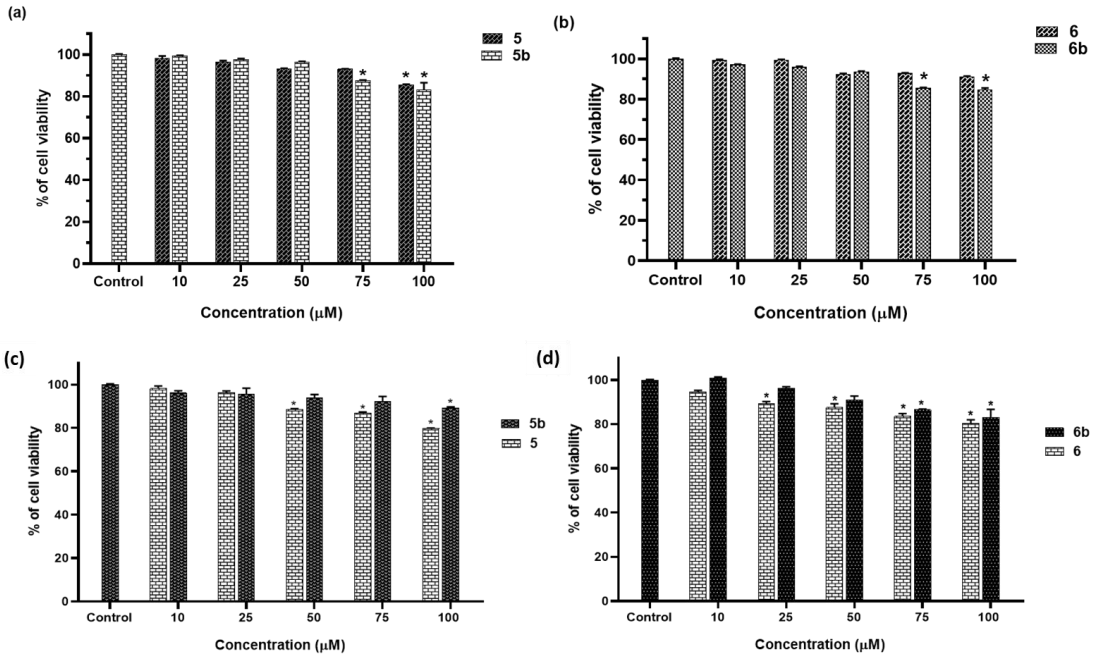

Figure 5.5. Cell viability assay of (a, c) compounds **5** and **5b**, and (b, d) compounds **6** and **6b** against MDA-MB-231 and HEK-293 cells, respectively, at various concentration ranging from 10 μM to 100 μM. Statistical analysis has been done by one-way ANOVA followed by Tukey's test where * denotes significant difference ($p<0.05$).

5.2.6. Cellular Uptake and Fluorescence Imaging Studies on molecules

With excellent spectral properties and good biocompatibility, the cellular uptake of compounds **5b and 6b** was explored and compared with **5** and **6** in MDA-MB-231 cell lines by fluorescence phase contrast microscope, respectively (figure 5.6). The images were captured in green channel (λ_{ex}: 470 nm; λ_{em}: 510-542 nm) and merged with phase contrast microscopic images. It was observed from the obtained images that compounds **5b** and **6b** are fairly internalized by the cancer cells. Also, the luminogenic intensity elicited by the green channel images of compounds **5b and 6b** was found to be more as compared to compounds **5 and 6,** respectively**.** Furthermore, the cellular uptake of the molecules by live breast cancer cells MDA-MB-231 was quantitatively measured by flow cytometry. The obtained results displayed that dyes **5b** and **6b**, having cyclobutylamine auxochrome, exhibited significantly higher cellular uptake in MDA-MB-231 cells compared to their respective reference **5** and **6**, having azetidine auxochrome (figure 5.7). These results demonstrated that cyclobutylamine moiety in comparison to azetidine improves the cell permeability of naphthalimide and nitrobenzoxadiazole dyes.

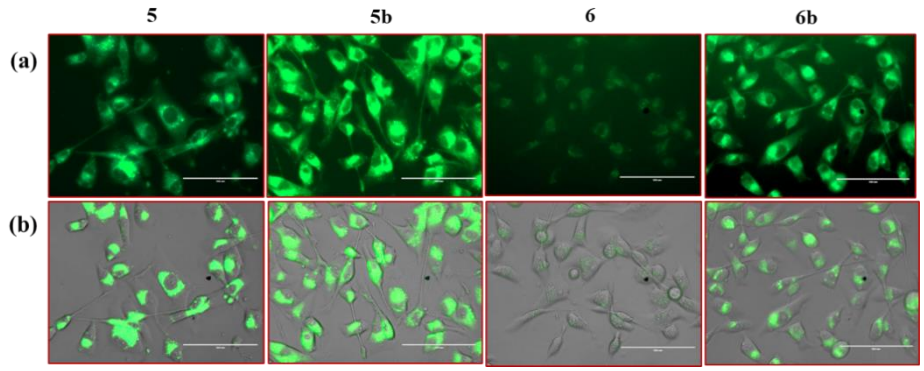

Figure 5.6. Illustration of fluorescence displayed by dyes **5**, **5b**, **6** and **6b** in MDA-MB-231 cell line captured with the help of inverted fluorescence phase contrast microscope at 400X magnification (a) in green channel (λ_{ex}: 470 nm; λ_{em}: 510-542 nm) and (b) overlay. Scale bar: 100 μm.

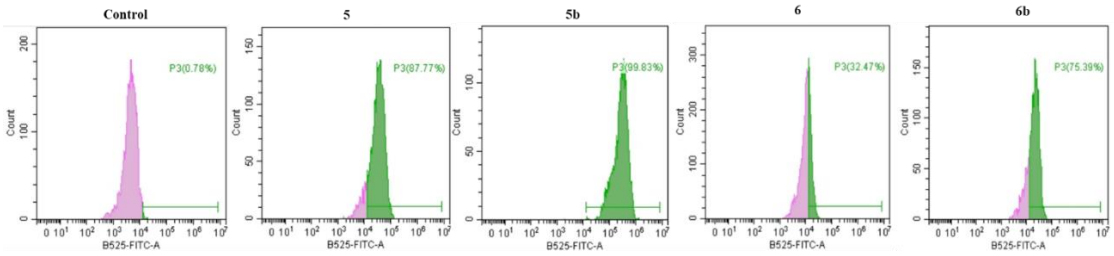

Figure 5.7. Comparison of average fluorescence intensity of dyes **5**, **5b**, **6** and **6b** with respect to control determined through flow cytometry in MDA-MB-231 cell lines after 30 minutes of incubation at 10 μM concentration.

5.3. Conclusion

In summary, cycloalkylamine substituted naphthalimides (**5a-5e)** and 4-nitrobenzoxadiazole (**6a-6e**) were synthesized and compared with azetidine substituted naphthalimide (**5**) and 4-nitrobenzoxadiazole (**6**) for their light-emitting properties, respectively. The photophysical studies exhibited that the cyclobutylaminated analogues **5b** and **6b** showed quantum yield and brightness higher than **5** and **6**, respectively. The quantum chemical calculations also corresponded to the practically obtained photophysical results. Compounds **5b** and **6b** were subjected to cytotoxicity assay in MDA-MB-231cells as well as non-cancerous HEK-293 cells, and the results indicated their biocompatibility in both the cell lines. Compounds **5b** and **6b** also showed excellent cell penetration, and better photostability compared to **5** and **6**, respectively.

5.4. Experimental section

5.4.1. Materials and methods

All chemicals were purchased from Sigma-Aldrich, TCI Chemicals, SRL Chemicals, and Avra, and used as received. Molychem silica gel (60-120 mesh) was used for column chromatography, and thin-layer chromatography was performed on Merck pre-coated silica gel 60-F254 plates. All other chemicals and solvents were obtained from commercial sources and

purified using standard methods. The characteristic FTIR spectra of the functional groups present in the synthesized molecules were obtained using Bruker Alpha ATR instrument. The ^{1}H NMR and ^{13}C NMR spectra were recorded on Bruker-Advance 500 and 600 MHz spectrometers. Chemical shifts (δ) are reported in parts per million (ppm), using TMS (δ = 0) as an internal standard and $CDCl_3$ and d^6-DMSO as NMR solvents. The mass spectrum of the compounds has been obtained by Waters Q-ToF Premier Mass Spectrometer. UV absorbance was measured on Agilent Cary UV 60 UV-Visible Spectrophotometer. Fluorescence data were recorded on a Molecular Devices SpectraMax M5 multimode plate reader. Solvent used for fluorescence spectra: Dichloromethane (DCM), Methanol (MeOH) and PBS, 1X (SRL Chemicals). GraphPad Prism ver. 7.0a (GraphPad Software, Inc.) was used to analyze data and generate graphs.

5.4.2. Photophysical Characterization

Maximum absorption wavelengths (λ_{abs}) of all the compounds were recorded using Agilent Cary UV 60 UV–Visible Spectrophotometer. Molar absorption coefficients (ε) were quantified using solutions of compounds **5-5e** and **6-6e** at concentrations ranging between 10^{-6} - 10^{-5} M in PBS (1X) by direct application of the Beer-Lambert's law. The compound stock solutions were prepared using DMSO (2 mL) and then diluted with PBS (upto 100 mL). Maximum emission wavelengths (λ_{em}) were recorded on a Horiba Scientific FluoroMax-4. λ_{abs} and λ_{em} were recorded in three solvents, namely, Dichloromethane (DCM), Methanol (MeOH) and Phosphate buffer [PBS, pH = 7.4] (SRL Chemicals) (table S1). All measurements were taken at ambient temperature (22 ± 2 °C) using 1-cm path length, 4 mL quartz cuvettes. GraphPad Prism ver. 7.0a (GraphPad Software, Inc.) was used to analyze all the data and generate the corresponding graphs. The spectral data have been normalized for better understanding (figure S5.1).

5.4.3. Absolute Quantum Yield (φ) Measurement

Absorbance spectra for each sample at a single concentration with an absorbance ranging between 0.07 and 0.09 were recorded. Absolute quantum yields (φ) of compounds **5-5e** and **6-6e** were measured employing a PTI K-Sphere petite Integrating sphere and quantum yield calculations were done through Horiba PTI Fluorescence Quanta Master 400 Systems. During measurement of φ with the instrument, samples (in 1X PBS) and blank (only PBS) were loaded individually in a 1 cm quartz cuvette which was then mounted at the center of the integrating sphere. The integrating sphere ensures collection of all the emitted and scattered light rays from the fluorescent sample. Samples were excited at different wavelengths, depending on their respective absorption maxima, with the help of a 75 W Xe PTI arc lamp housing (A-1010 B). The accuracy of the instrument-generated spectral correction was recorded using the corrected emission spectra of Rhodamine 6G (φ in ethanol = 0.95).

5.4.4. Computational chemistry

Computational studies were performed with the help of Gaussian 09 software. Density functional theory (DFT) and time-dependent (TD)-DFT calculations were used to measure the spectral properties of compounds **5b** and **6b** using their azetidinyl counterparts (**5** and **6**) as the reference. Geometry optimizations for **5b** and **6b** in ground state (S_0) and in the first excited singlet state (S_1) were carried out employing the B3LYP functional with the 6-31++G(d,p) basis set. Energy minimum after ground state (S_0) geometry optimizations were ensured by frequency calculations. Solvent effects (water) were taken into consideration using the IEFPCM model. Evaluations of DFT and TD-DFT theory used to calculate the absorption and emission maxima along with the energy gap between S_0 and S_1 states are found to be in good agreement with the practically obtained spectroscopic data (table S5.2)

5.4.5. pH stability and Photostability study

For the pH stability study, the buffers having pH ranges 4-8 were prepared using deionized water following standard protocol and freshly used. Compound **5**, **5b**, **6** and **6b** in a fixed concentration was placed in each buffer system and incubated for 30 mins at 37 ^{o}C before measuring the fluorescence intensities. For photostability tests, the compounds **5**, **5b**, **6**, **6b** and standard **coumarin 6** were dissolved in DMSO:PBS mixture, in a volume ratio of 20:80 in separate vials, and placed under continuous irradiation with a 500W tungsten lamp emitting white light. Their emission intensities were then measured after 0, 15, 30, 45, 60, 90, 120, 180, 240 and 300 minutes of irradiation and the obtained fluorescence intensities were plotted into a curve against time.

5.4.6. Cell culture and conditions

MDA-MB-231 type of breast cancer cell lines and human embryonic kidney 293 (HEK-293) cells were secured from the National Centre for Cell Science (NCCS), Pune, India. DMEM (Dulbecco's Modified Eagle Medium) was chosen as the cell culture medium, and was purchased along with 12 well cell culture plate from Genetics (Genetics Biotech Asia Pvt. Ltd). The T-25 flasks and 96 well plates were procured from Eppendorf. Other growth media essentials, such as Streptomycin, Penicillin, Trypsin-EDTA, and Fetal Bovine Serum (FBS) were purchased from Gibco. Phosphate Buffer Saline (PBS) was prepared using high grade analytical chemicals. The cells were cultured in FBS and penicillin-streptomycin supplemented DMEM and grown in a humidified CO_2 incubator at 37^{o}C.

5.4.7. Biocompatibility assay of compounds 5, 5b, 6 and 6b in cancer and non-cancer cells

Biocompatibility of compounds **5**, **5b**, **6** and **6b** against MDA-MB-231 cell line were analyzed in a 96-well cell culture plate, which contained 10,000 cells evenly distributed with onto the

entire plate, with each well containing 100 µl of the complete culture medium. The culture plate was then placed in a CO_2 incubator with 5% CO_2 at 37°C for 24 h to allow cells adherence. Following overnight incubation, the cells were treated with varying concentrations of each of the dyes **5**, **5b**, **6** and **6b** within a range of 10 - 100 µM and incubated for another 24 h. Cell viability was assessed by using MTT (3-(4,5-dimethylthiazol-2-yl)-2,5-diphenyltetrazolium bromide) assay. After 24 h of treatment, the MTT dye was re-constituted in phosphate buffered saline (PBS) and added to each of the wells and incubated for an additional 2 h at 37°C. The MTT-containing media was aspirated after 2 h, followed by the addition of 100 µl of DMSO in each well and subsequent incubation for another 30 mins to dissolve the purple-colored formazan precipitate. The plates were incubated for next 10 mins with gentle shaking. The optical density of each well was measured at 570 nm using a microplate reader. A similar protocol was followed for assay of compounds in HEK-293 cell lines.

5.4.8. Fluorescence imaging of treated cells and intracellular uptake assay

Approximately, 50,000 cells of MDA-MB-231 cell line were seeded in a 12 well culture plate and incubated for 24 h in a CO_2 incubator with 5% CO_2 at 37°C to ensure adherence. Followed by overnight incubation, the cells were treated with a concentration of 10 µM of each of the dyes **5**, **5b**, **6** and **6b** in complete DMEM for a standard duration of 30 minutes and incubated at 37^{o}C. Subsequently, the cells were washed with PBS and images were captured using an inverted fluorescence microscope in green channel at a 400 X magnification. The cellular uptake of the dyes was quantitatively measured using flow cytometry. For this, the MDA-MB-231 cells were treated with separately with dyes **5**, **5b**, **6** and **6b** and incubated for 30 mins. After incubation, the cells were harvested using 1 mM EDTA in PBS and processed further for experimentation through flow cytometry (Beckman Coulter) for the measurement of fluorescence intensities. The experiment was performed in triplicate.

5.4.9. Synthetic procedures of compounds 5-5e and 6-6e.

5.4.9.1. Procedure of synthesis of precursor B

A 10 ml round bottomed flask was charged with 6-bromo-1*H*,3*H*-benzo[de]isochromene-1,3-dione (**A,** 1.65 g, 6 mmol) and *n*-butylamine (2.5 equiv.) in ethanol (7 ml) as solvent and refluxed at 80 ºC for 2 h. After cooling the reaction mixture to ambient temperature, the solvent was evaporated *in vacuo* and the crude mixture was then diluted with water (20 mL) and extracted with ethyl acetate (25 mL ×3). After drying with anhydrous Na_2SO_4, the organic phase was evaporated to dryness and purified by column chromatography using 15% ethyl acetate: hexane as eluent to yield **B** (1.48 g, 75% yield) as a white solid.

5.4.9.2. General procedure of synthesis of 5-5e

Compound **B** (0.9 mmol, 1 equiv.) and the alicyclic amines or azetidine (1.5 equiv.) were weighed and placed in a 50 ml round bottomed flask containing 2 ml of DMSO. To this mixture triethylamine (1.5 equiv.) was added as a base and the reaction mixture was stirred at 110 ºC for 6 h. After cooling the reaction mixture to ambient temperature, the crude mixture was then diluted with water (10 mL) and extracted with ethyl acetate (15 mL ×3). After drying with anhydrous Na_2SO_4, the organic phase was evaporated to dryness and purified by column chromatography to obtain pure product.

5.4.9.3. General procedure of synthesis of 6-6e

4-chloro-7-nitrobenzo[c][1,2,5]oxadiazole **(C,** 1 mmol, 1 equiv.) and the alicyclic amines or azetidine (1.5 equiv.) were weighed and placed in a 50 ml round bottomed flask containing 2 ml of DMSO. To this mixture triethylamine (1.5 equiv.) was added as a base and the reaction mixture was stirred at room temperature for 2 h. After 2 h, the completion was confirmed by TLC and the crude mixture was diluted with water (10 mL) and extracted with ethyl acetate

(15 mL ×3). After drying with anhydrous Na_2SO_4, the organic phase was evaporated to dryness and purified by column chromatography to obtain pure product.

5.4.10. Spectral data of compounds 5-5e and 6-6e.

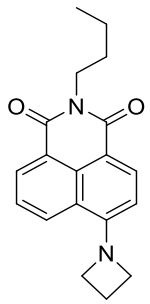

6-(azetidin-1-yl)-2-butyl-1H-benzo[de]isoquinoline-1,3(2*H*)-dione (5): The representative general procedure mentioned above was followed. The compound was purified by column chromatography using 15% ethyl acetate:hexane. Compound **5** was obtained as orangish yellow solid with 85 % yield. m.p.- 130 -134 ºC. FTIR (ATR): ν_{max} 2951, 2359, 1667, 1631, 1415, 1299, 1080, 1577, 799, 755 cm^{-1}. ^1H NMR (500 MHz, $CDCl_3$) δ 8.47 (d, *J* = 7.5 Hz, 1H), 8.32 (d, *J* = 8.5 Hz, 1H), 8.16 (d, *J* = 8.5 Hz, 1H), 7.43 (t, *J* = 7.5 Hz, 1H), 6.32 (d, *J* = 8.0 Hz, 1H), 4.42 (t, *J* = 7.5 Hz, 4H), 4.09 (t, *J* = 7.5 Hz, 2H), 2.50 (quint, *J* = 7.5 Hz, 1H), 1.67 – 1.60 (m, 2H), 1.40 – 1.33 (m, 2H), 0.90 (t, *J* = 7.5 Hz, 3H). ^{13}C NMR (125 MHz, $CDCl_3$) δ 164.7, 164.1, 152.57, 133.2, 131.1, 130.5, 129.9, 123.7, 122.8, 120.9, 110.4, 106.4, 106.3, 55.4, 40.0, 30.3, 20.4, 17.1, 13.8. HRMS (ESI) m/z calculated for $C_{19}H_{20}O_2N_2$ $[M + H]^+$ calculated as 309.1598, found 309.1615.

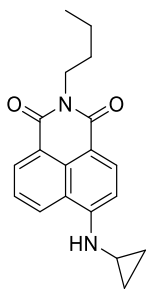

2-butyl-6-(cyclopropylamino)-1H-benzo[de]isoquinoline-1,3(2H)-dione (5a): The representative general procedure mentioned above was followed. The compound was purified by column chromatography using 10% ethyl acetate:hexane. Compound **5a** was obtained as greenish yellow solid with 75% yield. m.p.- 132 -134 ºC. FTIR (ATR): ν_{max} 2980, 2358, 1578, 1521, 1351, 1220, 803, 765 cm^{-1}. ^1H NMR (600 MHz, $CDCl_3$) δ 8.48 (d, *J* = 7.2 Hz, 1H), 8.41 (d, *J* = 8.4 Hz, 1H), 7.96 (d, *J* = 8.4 Hz, 1H), 7.50 (t, *J* = 8.4 Hz, 1H), 5.65 (s, 1H), 4.08 (t, *J* = 7.8 Hz, 1H), 2.64 – 2.60 (m, 1H), 1.65 (quint, *J* = 7.8 Hz, 3H), 1.36 (m, 2H), 0.92 – 0.89 (m, 4H), 0.65 – 0.63 (m, 2H). ^{13}C NMR (151 MHz, $CDCl_3$) δ 163.7, 163.2, 149.0, 133.1, 130.0, 128.5, 124.7, 123.7, 122.1, 119.1, 110.1, 105.1, 39.0, 29.3, 24.1, 19.4, 12.8, 6.8. HRMS (ESI) m/z calculated for $C_{19}H_{20}O_2N_2$ $[M + H]^+$ calculated as 309.1598, found 309.1615.

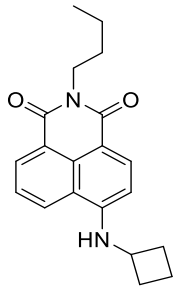

2-butyl-6-(cyclobutylamino)-1H-benzo[de]isoquinoline-1,3(2H)-dione (5b): The representative general procedure mentioned above was followed. The compound was purified by column chromatography using 15% ethyl acetate:hexane. Compound **5b** was obtained as yellow solid with 78% yield. m.p.- 149 -152 ºC. FTIR (ATR): ν_{max} 3348, 2944, 2358, 1574, 1527, 1382, 1231, 1131, 756 cm^{-1}. ^1H NMR (500 MHz, $CDCl_3$) δ 8.58 (d, *J* = 7.5 Hz, 1H), 8.44 (d, *J* = 8.5 Hz, 1H), 8.07 (d, *J* = 8.5 Hz, 1H), 7.62 (t, *J* = 8Hz, 1H), 6.62 (d, *J* = 8 Hz, 1H), 5.36 (d, *J* = 5Hz, 1H), 4.22 – 4.14 (m, 3H), 2.64 – 2.59 (m, 2H), 2.07 – 1.92 (m, 4H), 1.71 (q, *J* = 7.5 Hz, 2H), 1.47 – 1.40 (m, 2H), 0.96 (t, *J* = 7.5 Hz, 3H). ^{13}C NMR (125 MHz, $CDCl_3$) δ 164.7, 164.1, 148.1, 134.3, 131.0, 129.8, 125.7, 124.7, 123.3, 120.1, 110.7, 105.1,

48.6, 39.9, 30.8, 30.3, 20.4, 15.5, 13.8. HRMS (ESI) m/z calculated for $C_{20}H_{22}O_2N_2$ $[M + H]^+$ calculated as 323.1754, found 323.1756.

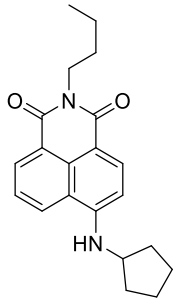

2-butyl-6-(cyclopentylamino)-1H-benzo[de]isoquinoline-1,3(2H)-dione (5c): The representative general procedure mentioned above was followed. The compound was purified by column chromatography using 12.5 % ethyl acetate:hexane. Compound **5c** was obtained as red solid with 75% yield. m.p.- 142 - 144 ^oC. FTIR (ATR): ν_{max} 3370, 2938, 2864, 2358, 1575, 1345, 1253, 1180, 925, 761 cm^{-1}. ^1H NMR (500 MHz, $CDCl_3$) δ 8.53 (dd, *J* = 7.5 Hz, 1Hz, 1H), 8.42 (d, *J* = 8.5 Hz, 1H), 8.07 (dd, *J* = 8.5 Hz, 1Hz, 1H), 7.56 - 7.53 (m, 1H), 6.72 (d, *J* = 8.5 Hz, 1H), 5.36 (d, *J* = 0.5 Hz, 1H), 4.15 (t, *J* = 7.5 Hz, 2H), 2.23 – 2.17 (m, 2H), 1.83 – 1.63 (m, 8H), 1.47 – 1.39 (m, 2H), 0.96 (t, *J* = 8 Hz, 3H). ^{13}C NMR (125 MHz, $CDCl_3$) δ 164.7, 164.4, 149.0, 134.3, 130.9, 129.8, 125.8, 124.5, 123.1, 120.2, 110.0, 105.2, 54.6, 39.9, 33.4, 30.3, 24.2, 20.4, 13.8. HRMS (ESI) m/z calculated for $C_{21}H_{24}O_2N_2$ $[M + H]^+$ calculated as 337.1911, found 337.1918

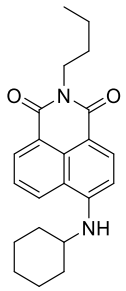

2-butyl-6-(cyclohexylamino)-1H-benzo[de]isoquinoline-1,3(2H)-dione (5d): The representative general procedure mentioned above was followed. The compound was purified

by column chromatography using 10% ethyl acetate:hexane. Compound **5d** was obtained as yellowish orange with 74% yield. m.p.- 135 -137 ºC. FTIR (ATR): ν_{max} 3346, 2973, 2359, 1577, 1344, 1236, 803, 760 cm^{-1}. ^{1}H NMR (600 MHz, $CDCl_3$) δ 8.44 (d, *J* = 7.2 Hz, 1H), 8.33 (d, *J* = 8.4 Hz, 1H), 8.00 (d, *J* = 8.4 Hz, 1H), 7.45 (t, *J* = 7.8 Hz, 1H), 6.63 (d, *J* = 8.4 Hz, 1H), 5.23 (s, 1H), 4.07 (t, *J* = 7.8 Hz, 2H), 3.54 -3.49 (m, 1H), 2.10 (d, *J* = 10.8 Hz, 2H), 1.77 – 1.75 (m, 2H), 1.65 – 1.59 (m, 3H), 1.42 -.1.16 (m, 7H), 0.87 (t, *J* = 7.8 Hz, 3H). ^{13}C NMR (151 MHz, $CDCl_3$) δ 163.6, 163.0, 147.4, 133.4, 130.0, 128.9, 124.8, 123.4, 122.0, 119.1, 108.6, 103.5, 50.7, 38.9, 31.7, 29.3, 24.6, 23.8, 19.4, 12.8. HRMS (ESI) m/z calculated for $C_{22}H_{26}O_2N_2$ $[M + H]^+$ calculated as 351.2067, found 351.2071.

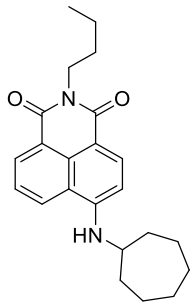

2-butyl-6-(cycloheptylamino)-1H-benzo[de]isoquinoline-1,3(2H)-dione (5e): The representative general procedure mentioned above was followed. The compound was purified by column chromatography using 10 % ethyl acetate:hexane. Compound **5e** was obtained as orangish brown solid with 68 % yield. m.p.- 130 -134 ºC. FTIR (ATR): ν_{max} 2963, 2359, 1577, 1539, 1343, 1255, 797, 765 cm^{-1}. ^{1}H NMR (600 MHz, $CDCl_3$) δ 8.46 (d, *J* = 7.2 Hz, 1H), 8.35 (d, *J* = 8.4 Hz, 1H), 8.00 (d, *J* = 8.4 Hz, 1H), 7.47 (t, *J* = 7.8 Hz, 1H), 6.54 (d, *J* = 8.4 Hz, 1H), 5.25 (d, *J* = 6.6 Hz, 1H), 4.07 (t, *J* = 7.8 Hz, 2H), 3.71 -3.65 (m, 1H), 2.07 – 2.04 (m, 2H), 1.69 – 1.50 (m, 12H), 1.38 – 1.32 (m, 2H), 0.88 (t, *J* = 7.8 Hz, 3H). ^{13}C NMR (151 MHz, $CDCl_3$) δ 163.6, 163.1, 147.2, 133.4, 130.0, 128.9, 124.8, 123.4, 122.1, 119.2, 108.7, 103.7, 52.7, 38.9, 33.5, 29.3, 27.1, 23.3, 19.4, 12.8. HRMS (ESI) m/z calculated for $C_{23}H_{28}O_2N_2$ $[M + H]^+$ calculated as 365.2224, found 365.2232.

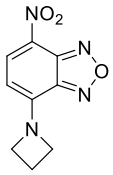

4-(azetidin-1-yl)-7-nitrobenzo[*c*][1,2,5]oxadiazole (6): The representative general procedure mentioned above was followed. The compound was purified by column chromatography using 30 % ethyl acetate:hexane. Compound **6** was obtained as dark brown crystalline solid with 67 % yield. m.p.- 210 - 212 ºC. FTIR (ATR): ν_{max} 2978, 2872, 2359, 1576, 1485, 1261, 1186, 798 cm^{-1}. ^{1}H NMR (500 MHz, d_6-DMSO) δ 8.45 (d, J = 9 Hz, 1H), 6.03 (d, J = 9 Hz, 1H), 4.76 (s, 2H), 4.41 (s, 2H), 2.25 (t, J = 7.5 Hz, 2H). ^{13}C NMR (125 MHz, d_6-DMSO) δ 145.6, 145.0, 144.1, 136.8, 99.9, 56.9, 53.4, 17.0. HRMS (ESI) m/z calculated for $C_9H_8O_3N_4$ $[M + H]^+$ calculated as 221.0669, found 221.0662.

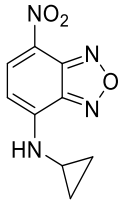

***N*-cyclopropyl-7-nitrobenzo[*c*][1,2,5]oxadiazol-4-amine (6a):** The representative general procedure mentioned above was followed. The compound was purified by column chromatography using 28 % ethyl acetate:hexane. Compound **6a** was obtained as dark greenish brown crystalline solid with 67 % yield. m.p.- 123 - 127 ºC. FTIR (ATR): ν_{max} 2976, 2870, 2347, 1559, 1488, 1186, 1137, 773 cm^{-1}. ^{1}H NMR (500 MHz, $CDCl_3$) δ 8.52 (d, J = 8.5 Hz, 1H), 6.63 (s, 1H), 6.59 (d, J = 9.0 Hz, 1H), 2.86 - 2.83 (m, 1H), 1.09 – 1.06 (m, 2H), 0.88 – 0.84 (m, 2H). ^{13}C NMR (125 MHz, $CDCl_3$) δ 144.6, 144.1, 143.8, 136.2, 124.6, 100.4, 25.2, 7.7. HRMS (ESI) m/z calculated for $C_9H_8O_3N_4$ $[M + H]^+$ calculated as 221.0669, found 221.0662.

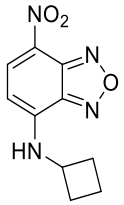

***N*-cyclobutyl-7-nitrobenzo[*c*][1,2,5]oxadiazol-4-amine (6b):** The representative general procedure mentioned above was followed. The compound was purified by column chromatography using 25 % ethyl acetate:hexane. Compound **6b** was obtained as dark red solid with 65 % yield. m.p.- 120 - 125 ºC. FTIR (ATR): ν_{max} 2936, 2866, 2356, 1732, 1487, 1185, 829 cm^{-1}. ^{1}H NMR (500 MHz, $CDCl_3$) δ 8.45 (d, *J* = 9 Hz, 1H), 6.59 (d, *J* = 4 Hz, 1H, NH), 6.10 (d, *J* = 8.5 Hz, 1H), 4.30 (d, *J* = 6 Hz, 1H), 2.64 – 2.58 (m, 2H), 2.24 – 2.16 (m, 2H), 2.03 – 1.91 (m, 2H). ^{13}C NMR (125 MHz, $CDCl_3$) δ 144.1, 143.9, 142.6, 136.5, 123.8, 99.2, 44.8, 30.2, 15.5. HRMS (ESI) m/z calculated for $C_{10}H_{10}O_3N_4$ $[M + H]^+$ calculated as 235.0826, found 235.0820.

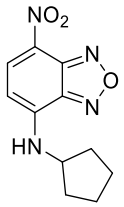

***N*-cyclopentyl-7-nitrobenzo[*c*][1,2,5]oxadiazol-4-amine (6c):** The representative general procedure mentioned above was followed. The compound was purified by column chromatography using 25% ethyl acetate:hexane. Compound **6c** was obtained as brownish solid with 60 % yield. m.p.- 105 -110 ºC. FTIR (ATR): ν_{max} 2975, 2871, 2359, 1563, 1486, 1290, 804, 742 cm^{-1}. ^{1}H NMR (500 MHz, $CDCl_3$) δ 8.48 (d, *J* = 8.5 Hz, 1H), 6.34 (d, *J* = 5 Hz, 1H, NH), 6.21 (d, *J* = 8.5 Hz, 1H), 4.16 (d, *J* = 3.5 Hz, 1H), 2.26 – 2.22 (m, 2H), 1.90 - 1.75 (m, 6H). ^{13}C NMR (125 MHz, $CDCl_3$) δ 144.3, 143.9, 143.4, 136.5, 123.6, 99.2, 55.4, 33.1,

24.1. HRMS (ESI) m/z calculated for $C_{11}H_{12}O_3N_4$ $[M + H]^+$ calculated as 249.0982, found 249.0982.

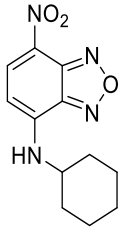

***N*-cyclohexyl-7-nitrobenzo[*c*][1,2,5]oxadiazol-4-amine (6d):** The representative general procedure mentioned above was followed. The compound was purified by column chromatography using 20% ethyl acetate:hexane. Compound **6d** was obtained as blackish green solid with 69 % yield. m.p.- 144 - 149 ºC. FTIR (ATR): ν_{max} 2944, 2869, 2355, 1585, 1485, 1227, 1139, 793, 739 cm^{-1}. ^1H NMR (500 MHz, $CDCl_3$) δ 8.49 (d, *J* = 9.0 Hz, 1H), 6.23 (d, *J* = 8.0 Hz, 1H), 6.21 (d, *J* = 8.5 Hz, 1H), 3.72 (s, 1H), 2.19 – 2.17 (m, 2H), 1.91 – 1.87 (m, 2H), 1.77 -1.68 (m, 2H), 1.53 – 1.43 (m, 4H). ^{13}C NMR (125 MHz, $CDCl_3$) δ 144.3, 144.0, 142.9, 136.6, 123.4, 98.6, 52.9, 32.2, 25.2, 24.5. HRMS (ESI) m/z calculated for $C_{12}H_{14}O_3N_4$ $[M + H]^+$ calculated as 263.1139, found 263.1130.

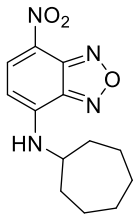

***N*-cycloheptyl-7-nitrobenzo[*c*][1,2,5]oxadiazol-4-amine (6e):** The representative general procedure mentioned above was followed. The compound was purified by column chromatography using 20% ethyl acetate:hexane. Compound **6e** was obtained as blackish green solid with 69 % yield. m.p.- 102 -106 ºC. FTIR (ATR): ν_{max} 2359, 1567, 1489, 1250, 801 cm^{-1}. ^1H NMR (500 MHz, $CDCl_3$) δ 8.50 (d. *J* = 8.5 Hz, 1H), 6.27 (d. *J* = 7.0 Hz, 1H), 6.13 (d. *J*

= 8.5 Hz, 1H), 3.85 (s, 1H), 2.19 – 2.15 (m, 2H), 1.81 – 1.62 (m, 10H). ^{13}C NMR (125 MHz, $CDCl_3$) δ 144.4, 144.0, 142.6, 136.5, 123.6, 98.8, 55.0, 34.2, 27.9, 24.1. HRMS (ESI) m/z calculated for $C_{13}H_{16}O_3N_4$ $[M + H]^+$ calculated as 277.1295, found 277.1305.

5.5. References

(1) Jain, N.; Kaur, N. A Comprehensive Compendium of Literature of 1,8-Naphthalimide Based Chemosensors from 2017 to 2021. *Coord. Chem. Rev.* **2022**, *459*, 214454. https://doi.org/10.1016/j.ccr.2022.214454.

(2) Yu, H.; Guo, Y.; Zhu, W.; Havener, K.; Zheng, X. Recent Advances in 1,8-Naphthalimide-Based Small-Molecule Fluorescent Probes for Organelles Imaging and Tracking in Living Cells. *Coord. Chem. Rev.* **2021**, *444*, 214019. https://doi.org/10.1016/j.ccr.2021.214019.

(3) Chen, J.; Wang, C.; Liu, W.; Qiao, Q.; Qi, H.; Zhou, W.; Xu, N.; Li, J.; Piao, H.; Tan, D.; Liu, X.; Xu, Z. Stable Super-Resolution Imaging of Lipid Droplet Dynamics through a Buffer Strategy with a Hydrogen-Bond Sensitive Fluorogenic Probe. *Angew. Chem. Int. Ed.* **2021**, *60* (47), 25104–25113. https://doi.org/10.1002/anie.202111052.

(4) Jiang, C.; Huang, H.; Kang, X.; Yang, L.; Xi, Z.; Sun, H.; Pluth, M. D.; Yi, L. NBD-Based Synthetic Probes for Sensing Small Molecules and Proteins: Design, Sensing Mechanisms and Biological Applications. *Chem. Soc. Rev.* **2021**, *50* (13), 7436–7495. https://doi.org/10.1039/D0CS01096K.

(5) Grimm, J. B.; English, B. P.; Chen, J.; Slaughter, J. P.; Zhang, Z.; Revyakin, A.; Patel, R.; Macklin, J. J.; Normanno, D.; Singer, R. H.; Lionnet, T.; Lavis, L. D. A General Method to Improve Fluorophores for Live-Cell and Single-Molecule Microscopy. *Nat. Methods* **2015**, *12* (3), 244–250. https://doi.org/10.1038/nmeth.3256.